

How does the hydrocracking bifunctional catalyst work on the selectivity of Middle Distillate (MD) and the conversion of Vacuum Gas Oil (VGO) Hydrocracking?

Melaz Tayakout-Fayolle,^{a*} Barbara Browning,^a Isabelle Pitault,^a Françoise Couenne,^a

^a Univ Lyon, Université Claude Bernard Lyon 1, CNRS, LAGEP UMR 5007, 43 boulevard du 11 novembre 1918, F-69100, VILLEURBANNE, France

*Corresponding author: Email: melaz.tayakout-fayolle@univ-lyon1.fr

Abstract: A kinetic model for hydrocracking of a real VGO feedstock defined by hydrocarbon families and carbon number has been extended to 8 different zeolite and metal loadings. The geometry of the zeolite crystallites within the catalyst structure is taken into account to describe the different loadings. This geometry is a new structural parameter which allows to understand how the catalyst works. This model gave good agreement between calculated and measured lump mass fractions, conversions and selectivities.

Keywords: bifunctional catalyst, GC x GC, hydrocracking kinetic modelling, structural parameter

1. Introduction

A typical hydrocracking process of VGO is carried out over a bifunctional catalyst in a trickle bed reactor operating under high temperature and pressure, between 340°C and 450°C and 80 to 180 bars. The bifunctional catalyst contains Brønsted acid sites which catalyze the cracking and isomerisation reactions and metallic sites for hydrogenation/dehydrogenation. Conversion and selectivity depend strongly on catalyst homogeneity and the relative quantities of acidic and metallic sites¹. The almost works in the literature used a distribution approach with the reaction mixture represented by boiling ranges and a correlation for hydrocracking rate as a function of TBP. Browning et al.^{2,3} have developed an alternative approach based on 217 discrete lumps classified by carbon number provided by GC x GC and hydrocarbon family and a distribution approach to define the kinetic parameters.

2. Experimental and Theoretical

Hydrocracking experiments have been carried out with a VGO in a laboratory scale batch reactor and using several catalysts with different ratios of zeolite to metal sites under conditions close to those found in industrial units. Experimental campaign is described in the work of R. Henry et al.⁴. The model, described in detail in Browning et al.² and validated for the reference catalyst ($C_1^{0.7}$) has been used to simulate the hydrocracking experiments⁴. The model inputs are the metal mass loading, the zeolite mass, the initial liquid and vapour phase compositions at time t_0 (the moment when the reactor reaches operating conditions) and the hydrogen feed rate. A new input is necessary to take the catalyst geometry into account when the ratio between zeolite and metal sites varies. The structural parameter is a physical property of the catalyst and shows how the catalyst works.

3. Results and discussion

Structural parameter: the first stage of catalyst fabrication is to mix zeolite crystallites and alumina precursor. The metallic sites are loaded later and attach mainly to the alumina. If the zeolite crystallites are assumed to be of the average size, uniformly distributed and having the same density and porosity as the surrounding alumina, then a pre-loading unit cube of zeolite and alumina can be defined as shown in Figure 1. L is the length of side of the cube, l_a and l_z are the length fractions of the unit cube. From the assumptions, the volume fraction of the unit cube taken up by the zeolite is equal to its pre-loading mass fraction, m_{z0} , and therefore its dimensions relative to the unit cube are known. The structural factor values are calculated from the relative lengths of the unit cube and m_{z0} as follows: $\sigma = \left(\frac{l_z}{l_a}\right) \left(\frac{1}{m_{z0}}\right)$. The distance between zeolite and metallic sites is in the range of 5.8 to 9 nm and the number of metal sites on a straight line between two

zeolite crystallites is in the range of 55 to 138nm. This result suggests the intimacy of the different active sites to be less important than the geometry and spacing of the zeolite crystallites. The distances between metallic sites are shorter than those between crystallites so the range of absolute distances tested is tiny compared to that for the zeolite and to be a potential reason why it may have had less impact.

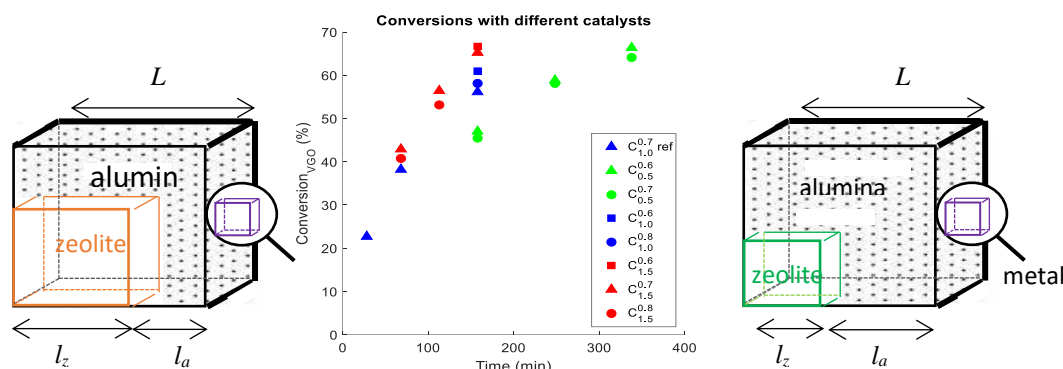


Figure 1. Unit cube of zeolite and alumina

As a consequence, the contact time defined in works of B. Browning et al.² should be amended to include the relative lengths in the unit cube as shown in Figure 1. Figure 2 shows that the VGO conversion (a) and selectivity in MD (b) plotted against the amended contact time gives a better grouping of the different catalysts used and the VGO conversion, respectively. The closer the conversion curves for the different catalysts are the more the kinetic parameters are independent of the catalyst properties.

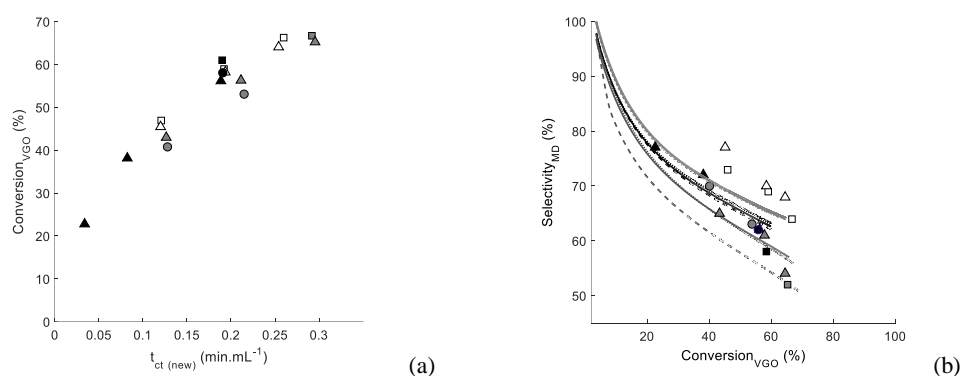


Figure 1. For all studied catalysts: VGO conversion (a) and selectivity (b) at 400 °C vs amended contact time and VGO conversion, respectively.

4. Conclusions

This kinetic model is capable of representing conversion and selectivity for VGO hydrocracking quite well. The fact that it captures the same trends as found in the experimental data for the other catalysts is very positive. Calculated cracking rates depend on the geometry of the catalyst, i.e. the distance between zeolite crystallites, the size of the crystallites and the fraction of metal in the zeolite alumina matrix. Nevertheless, the model underestimates MD selectivity and therefore must overestimate cracking rates to some degree. Catalyst metal loading is known to impact selectivity and is taken into account in the model. This difference between the calculation results and the measured data is probably due to an overestimation of the amount of overcracking (cracking of MD).

References

1. J.W. Thybaut, C.S. Laxmi Narasimhan, J.F. Denayer, G.V. Baron, P.A. Jacobs, J.A. Martens, G.B. Marin, *Ind. Eng. Chem. Res.* 44 (2005) 5159.
2. B. Browning, P. Afanasiev, I. Pitault, F. Couenne, M. Tayakout-Fayolle, *Chem. Eng. J.* 284 (2016) 270.
3. B. Browning, R. Henry, P. Afanasiev, G. Lapisardi, G. Pirngruber, M. Tayakout-Fayolle, *Ind. Eng. Chem. Res.* 53 (2014) 8311.
4. R. Henry, M. Tayakout-Fayolle, P. Afanasiev, C. Lorentz, G. Lapisardi, G. Pirngruber, *Catal. Today.* 220–222 (2014) 159.